Drug Delivery and Translational Research (2020) 10:826–837
https://doi.org/10.1007/s13346-020-00738-z

ORIGINAL ARTICLE

Zein nanoparticles as low-cost, safe, and effective carriers to improve the oral bioavailability of resveratrol

Rute Nunes[1,2] · Ana Baião[1,2] · Diana Monteiro[1,2] · José das Neves[1,2,3] · Bruno Sarmento[1,2,3]

Published online: 23 March 2020

Abstract

The clinical translation of the multiple pharmacological effects of resveratrol (RSV) found in preclinical studies has been impaired by its poor bioavailability, due to poor solubility and rapid metabolism and elimination. The inclusion of this molecule in medicines or functional food products will be ineffective unless suitable systems are developed. Zein protein may constitute an inexpensive, safe, and effective choice to produce nanoparticles (NPs) to incorporate hydrophobic molecules and overcome the bioavailability issues of RSV. In this work, we loaded RSV into zein NPs by using a nanoprecipitation method. Unloaded and RSV-loaded NPs presented average diameter values in the range of 120–180 nm, narrow size distribution (polydispersity index < 0.150), and zeta potential of around + 20 mV. The association efficiency of the drug was equal to or greater than 77% for different initial drug loads. Scanning electron microscopy imaging revealed that zein NPs were round-shaped and presented a smooth surface. Aqueous suspensions of zein NPs were stable for at least 1 month when stored at 4 °C. The freeze-drying of zein NPs using sucrose as cryoprotectant allowed an easy re-suspension of NPs in water without significantly changing the initial colloidal properties. RSV-loaded NPs presented low cytotoxicity to the human colorectal Caco-2 and HT29-MTX cell lines. Finally, permeability studies of RSV across Caco-2 and Caco-2/HT29-MTX evidenced some ability of zein NPs to protect RSV from metabolism events. However, further investigation is needed in order to confirm the possible role of zein NPs in the metabolic stability of RSV. Overall, zein NPs may present the potential to circumvent bioavailability issues of RSV.

Keywords Bioavailability · Drug delivery systems · Poorly soluble molecules · Protein-based nanoparticles

Introduction

The polyphenol resveratrol (RSV) has been receiving particular attention from the scientific and medical communities due to its potential pleiotropic effects on human health, including antioxidant, anti-inflammatory, cardio- and neuroprotective, and anticancer properties [1, 2]. Past research and development efforts focused mainly on the therapeutic use of RSV but this molecule is also a strong candidate for the inclusion on large human consumption products in order to take advantage of its potential biological effects. However, the use of RSV as a nutraceutical has been hampered by its low aqueous solubility, poor stability, and rapid metabolization by CYP 450 enzymes in the intestines and liver, resulting in poor bioavailability [3]. The use of nanotechnology-based systems may help to overcome many of the formulation challenges associated with RSV [4, 5]. The advantageous features of drug delivery nanosystems are plentiful and include the improvement in the solubility of poorly soluble molecules, the protection of the cargo from degradation, the ability to deliver the molecule in a sustained or controlled way, and the possibility of targeting different cells and/or tissues [6, 7]. Nanoparticles (NPs), in particular, have been widely explored as drug delivery systems for the improvement of the oral bioavailability of numerous molecules. They can be made of natural and synthetic polymers, lipids, or other materials such as proteins [6, 8–10]. Protein-based nanoparticles, in particular, are promising matrices for the development of drug delivery carriers but

Electronic supplementary material The online version of this article (https://doi.org/10.1007/s13346-020-00738-z) contains supplementary material, which is available to authorized users.

✉ Rute Nunes
rute.nunes@ineb.up.pt

[1] i3S – Instituto de Investigação e Inovação em Saúde, Universidade do Porto, Porto, Portugal

[2] INEB - Instituto de Engenharia Biomédica, Universidade do Porto, Porto, Portugal

[3] CESPU, Instituto de Investigação e Formação Avançada em Ciências e Tecnologias da Saúde, Gandra, Portugal

the number of proteins able to yield suitable nanosystems is scarce [11, 12]. Zein is a water-insoluble protein extracted from corn. It is classified as generally recognized as safe (GRAS) by the Food and Drug Administration (FDA) and is used as a coating material, extended-release agent, and tablet binder in pharmaceutical applications and as a coating agent in food applications [13]. The hydrophobicity of zein is attributed to the high proportion of hydrophobic amino acids (> 50%), turning this protein an attractive matrix to encapsulate hydrophobic compounds [14]. Also, zein possesses high thermal resistance and great oxygen barrier properties being an attractive matrix for the association of compounds sensitive to temperature and/or oxidation [15]. Therefore, the main aim of this work is to develop NPs suitable for loading RSV, in order to improve its stability and, ultimately, its oral bioavailability.

Materials and methods

Materials

Zein (38 kDa, content in protein 81.9–100%, calculated on a dry basis) was acquired from Sigma Aldrich (Sto. Louis, MO, USA). *Trans*-RSV 99% (pharmaceutical grade) was purchased from Abatra Technology Co., Ltd. (Xi'an, China) and ethanol (99.9%) from Merck Millipore (Darmstadt, Germany). Poloxamer P407 (Kolliphor® P 407) was kindly provided by BASF (BTCEurope, Barcelona, Spain). Ultrapure water was obtained in-house using a Milli-Q purification system (Merck Millipore). D-Sucrose (≥ 99.9%), D-trehalose (≥ 99.9%), D-fructose (≥ 99.9%), and D-glucose (Ph. Eur. grade) were obtained from Sigma-Aldrich (Steinheim, Germany). All other solvents and chemicals were of analytical grade or equivalent.

Production of RSV-loaded zein NPs

RSV-loaded zein NPs were produced by the nanoprecipitation technique. Briefly, RSV was dissolved in 1 mL of ethanol and added to 5 mL of a 70% (v/v) ethanol solution containing zein (20 mg mL^{-1}). This solution was magnetically stirred over 1 h at room temperature (500 rpm) and further added dropwise to 20 mL of water under magnetic stirring (200 rpm) by using a 1-mL micropipette. NPs were collected after 3 h of stirring at room temperature and centrifuged for 30-40 min through a filter device with a molecular weight cutoff of 30 kDa (Amicon Ultra filter, Ultracel membrane with 30,000 MWCO, Millipore Corporation, Bedford, MA, USA) at 3000×*g*. Milli-Q water was used to recover the NPs from the filter.

Particle size, polydispersity index, and zeta potential

Fresh unloaded and RSV-loaded NPs were dispersed in 10 mM NaCl (0.2 mg mL^{-1}) adjusted to pH 5.5 with HCL 0.5 M and characterized regarding size and size distribution by dynamic light scattering (DLS) and zeta potential (ZP) by laser Doppler electrophoresis using a Zetasizer Nano ZS (Malvern Instruments, Malvern, UK). All measurements were performed in triplicate at 25 °C.

Surface morphology

The surface morphology of zein NPs was assessed by scanning electron microscopy (SEM) on the high-resolution (Schottky) environmental scanning electron microscope Quanta 400FEG ESEM (FEI, Hillsboro, OR, USA). Freeze-dried NPs were mounted onto metal stubs with carbon tape and sputter-coated with a thin layer of gold/palladium using the SPI Module Sputter Coater equipment (Structure Probe, Inc., West Chester, PA, USA).

Association efficiency and drug loading

The association efficiency (AE) and drug loading (DL) of RSV after the production of NPs were determined by an indirect method, expressed by the following formulas:

$$AE\ (\%) = \frac{\text{Initial amount of RSV} - \text{Amount of RSV in filtrates}}{\text{Total amount of RSV}} \times 100$$

$$DL\ (\%) = \frac{\text{Initial amount of RSV} - \text{Amount of RSV in filtrates}}{\text{Amount of zein} + \text{RSV}} \times 100$$

In this method, the amount of RSV loaded into zein NPs was given by the difference between the initial amount of RSV used to produce the NPs and the remaining drug collected in the filtrates after NP concentration by centrifugation. The amount of drug recovered in the filtrates was assessed using a previously described HPLC-UV method with slight changes [16]. The chromatographic analysis was performed using a Shimadzu UFLC Prominence System (Shimadzu Corporations, Kyoto, Japan) coupled with an autosampler SIL-20AC, a degasser DGU-20A5, and SPD-20A detector. A reverse-phase analytical column SymmetryShield™ RP8, 3.5 μm particle size, 4.6 mm internal diameter × 15 cm length (Waters, Milford, CT, USA) was used at 30 °C. The mobile phase consisted of acetonitrile and water (35:65, v/v) and elution was performed in isocratic mode. The flow rate was maintained at 1 mL min^{-1} and the injection volume was 10 μL and 50 μL for technological assays and permeability studies,

respectively. RSV was detected at 307 nm with a retention time of 8.5 min. A stock solution of RSV was prepared in acetonitrile and stored at − 80 °C. RSV standard solutions were prepared daily from the stock solution in acetonitrile:water (50:50, v/v). Linearity was established in the ranges of 1–30 μg mL^{-1} and 0.1–7 μg mL^{-1} ($r^2 \geq 0.999$ for linear least squares regression) for technological and permeability studies, respectively.

Stability of RSV-loaded zein NPs

Liquid suspensions of unloaded and RSV-loaded zein NPs were stored at 4 °C for 30 days after production. The particle size, size distribution, and ZP were assessed, as well as the amount of RSV recovered from filtrates after centrifugation, as described above.

In vitro drug release of RSV-loaded NPs

The in vitro release of RSV from zein NPs was carried out in a phosphate buffer saline (PBS) at pH 6.8 in order to mimic the intestinal pH. The assay was performed over 24 h at 37 °C and 100 rpm in an incubator shaker (IKA KS 4000 ic control, IKA®-Werke GmbH & Co. KG, Staufen, Germany). Briefly, 2 mg of NPs (corresponding to 0.1 mg of RSV) was placed in 10-mL PBS. Samples of 0.5 mL were collected at different time points and the same volume was replaced with fresh pre-heated PBS. Aliquots were centrifuged at 15000×*g* for 10 min (Eppendorf Centrifuge 5417R, Eppendforf AG, Hamburg, Germany) and 4 °C before quantification by HPLC-UV.

Lyophilization of zein NPs

Zein NPs at a concentration of 1 mg mL^{-1} were freeze-dried using D-glucose, D-fructose, D-sucrose, and D-trehalose as cryoprotectants (10%, w/v). NPs without cryoprotectant were used as a control. Zein NP suspensions with or without cryoprotectants were placed into semi-stoppered glass vials with slotted rubber lids and frozen at − 80 °C for 12 h. Samples were then transferred to a Modulyo 4K freeze dryer (Edwards, Crawley, UK) at 0.09 mbar and freeze-dried for 72 h. Lyophilization was done at a condenser surface temperature of − 60 °C ± 5 °C. After lyophilization, NPs were reconstituted in the initial volume (5 mL) of ultrapure water. Samples were left under static conditions for 10 min at room temperature before undergoing homogenization by vigorous vortexing. An aliquot of NP suspension was dispersed in NaCl 10 mM and the size, size distribution, and ZP were assessed as described in "Particle size, polydispersity index, and zeta potential" section.

Cell lines and culture conditions

Human colonic epithelial Caco-2 cells (C2BBe1 clone) were purchased from the American Type Culture Collection (ATCC, Manassas, VA, USA) and used at passages 68–81. Human colonic epithelial HT29-MTX cells were kindly provided by Dr. T. Lesuffleur (INSERM U178, Villejuif, France) and used at passages 39–47. The cell lines were maintained in Dulbecco's modified Eagle's medium (DMEM) with ultraglutamine (Lonza, Vervieres, Belgium) supplemented with 10% (v/v) fetal bovine serum (Biochrom GmbH, Berlin, Germany), 100 U mL^{-1} penicillin and 100 μg mL^{-1} streptomycin (BioWest, Nuaillé, France), and 1% (v/v) non-essential amino acids, 100× concentrate (Gibco, Paisley, UK). Both cell lines were tested and negative for *Mycoplasma* spp. Hank's balanced salt solution (HBBS) used in permeability experiments was acquired from Gibco.

Cytotoxicity of RSV-loaded zein nanoparticles

The potential effects of RSV-loaded zein NPs in the viability of Caco-2 and HT29-MTX colorectal cell lines were assessed using the triazolyl blue tetrazolium bromide (MTT, Sigma-Aldrich, St. Louis, MO, USA) metabolic activity assay. Briefly, Caco-2 and HT-29 MTX cells were individually seeded in 96-well plates at 10,000 cells/well and allowed to attach for 24 h at 37 °C and 5% CO_2. In the day of the experiment, serial dilutions of NPs or free RSV in complete DMEM were added to triplicate wells of cells and incubated for 24 h at 37 °C in a 5% CO_2 air atmosphere. Media only and 1% (w/v) Triton X-100 were used as controls. After incubation, cells were washed twice with PBS pH 7.4 and 200 μL of MTT solution (0.5 mg mL^{-1} in complete medium) were added to each well and incubated at 37 °C and 5% CO_2 for 4 h in the dark. MTT was removed and 200 μL of DMSO was added. After the complete dissolution of formazan crystals, the absorbance was determined at 590 nm with 630 nm background deduction. The half-maximal cytotoxic concentration (CC_{50}) was calculated by plotting the cell viability percentage (or cytotoxicity) (*y*-axis) against the $\log_{10}$ concentration of RSV (*x*-axis) using the sigmoidal dose-response (variable slope) equation in Prism version 5.01 for Windows (GrahPad Software, San Diego, CA, USA).

Permeability of RSV-loaded zein NPs across colorectal cell lines

The permeability of RSV was assessed in Caco-2 and Caco-2/HT29-MTX cell monolayers. Briefly, Caco-2 or Caco-2/HT29-MTX cells in a proportion of 90:10 were seeded at final a density of 1×10^5 cells cm^{-2} onto 1.0 μm polyethylene terephthalate (PET) membrane inserts with a cell growth area of 1.12 cm^2 (Millicel®, Merck KGaA, Darmstadt, Germany) and allowed to grow for 21 days with medium being changed every other

day. The evolution of growth and integrity of mono- and co-culture monolayers were assessed by measuring the transepithelial electrical resistance (TEER) after every medium replacement using an EVOM^2 epithelial voltohmmeter equipped with a STX2 electrode (World Precision Instruments, Inc., Sarasota, FL, USA). The TEER value was calculated by subtracting the resistance of a blank (cell-free culture insert with the medium) and correcting for the surface area of the Transwell® cell culture support. On the day of the experiment, the medium was removed from the apical and basolateral compartments and the cells were washed twice with HBSS pre-heated to 37 °C. Fresh HBSS was added to both compartments and the system was allowed to equilibrate for 30 min at 37 °C. In the basolateral compartment, HBSS contained 0.2% (w/v) of poloxamer 407 in order to assure sink conditions. After that, the HBSS from the apical compartment was replaced with 0.5 mL of NPs or RSV dispersed in pre-warmed HBSS at a concentration of 100 μM (expressed as drug content). Aliquots of 200 μL were collected from basolateral compartments at defined time points and the initial volume was refilled with pre-heated HBSS containing 0.2% (w/v) of poloxamer 407. After the last time point, the medium was removed from both compartments of the Transwell system and cells were washed twice with HBSS pre-heated to 37 °C. The resistance was monitored before the experiment and at each time point to assure the viability and monolayer integrity during the entire assay. At the end of the experiment, the membrane was detached from the insert and the cell monolayer was destroyed with DMSO and assayed for RSV quantification by HPLC-UV. Apparent permeability (P_{app}) values were calculated according to the equation:

$$P\mathrm{app} = \frac{dQ}{dt}\ (A \times C0)$$

where dQ is the amount of RSV that permeated the monolayer, A is the diffusion area (cm^2), $C0$ is the initial concentration of RSV (μg cm^3), and dt is the total time of experiments. The coefficient dQ/dt represents the steady-state flux of RSV across the monolayer.

Statistical analysis

All results are presented as mean ± standard deviation (SD) unless otherwise mentioned. Two-tailed Student's t test was used to compare two independent groups. One-way analysis of variance was performed to compare multiple independent groups. When significantly different (p <0.05), differences between groups were compared with the post hoc tests Dunnett's, and Tukey's for viability and for permeability assays, respectively. Differences were considered significant for p <0.05.

Results and discussion

Characterization of RSV-loaded NPs

Zein NPs were successfully obtained by the nanoprecipitation technique. RSV was loaded in zein NPs at different theoretical loadings, namely 5%, 10%, and 15% (w/w). RSV-loaded NPs presented a mean hydrodynamic diameter between 130 and 190 nm, increasing with the increase of theoretical drug loading (Table 1). This may result from the association of higher amounts of RSV molecules within the zein matrix, causing an increase in the particle size. Low polydispersion index (PdI) values were obtained for all formulations, although a trend for higher values was observed when 10% and 15% of RSV were used. The histograms of size distribution by intensity and ZP curves are presented in Figure S1 and Figure S2, respectively, in Supplementary information. ZP values were around + 20 mV and high association efficiency values (> 70%) were obtained for all formulations. The positive charge of zein is expected at the pH of the dispersant media used for NP measurement (pH 5.5), since the isoelectric point of zein is around 6.2 [17, 18]. RSV will be neutral at this pH (p$Ka_{1,2,3}$ = 8.8, 9.8, 11.4) [19].

SEM images confirmed DLS results regarding the size and size distribution of zein NPs (Fig. 1a–d). Zein NPs featured round shape and smooth surface (Fig. 1a). The association of increasing amounts of RSV had no apparent impact on the morphology of zein NPs (Fig. 1b, d). Comparable properties between unloaded and drug-loaded NPs suggest that RSV was effectively entrapped within the polymeric matrix.

Furthermore, liquid suspensions of NPs were stored at 4 °C after production and the size, size distribution, and ZP were assessed after 30 days (Fig. 2). No significant changes were observed in size, size distribution, and ZP of unloaded zein NPs (Fig. 2a–c. In the case of NPs loaded with RSV, a decrease in size was noticed, although only significant in the case of 5%

Table 1 Hydrodynamic diameter (HD), polydispersity index (PdI), zeta potential (ZP), association efficiency (AE), and drug loading (DL) values of RSV-loaded NPs at different theoretical drug loadings. Results are presented as mean ± SD (n = 3)

Theoretical drug loading (%)	HD (nm)	PdI	ZP (mV)	AE (%)	DL (%)
0	129 ± 3	0.087 ± 0.017	19.4 ± 1.7	–	–
5	141 ± 7	0.081 ± 0.013	21.0 ± 1.6	77.6 ± 1.6	3.9 ± 0.1
10	166 ± 34	0.126 ± 0.064	23.9 ± 3.0	91.6 ± 0.6	9.2 ± 0.1
15	187 ± 7	0.133 ± 0.003	23.2 ± 1.0	92.5 ± 1.3	13.9 ± 0.2

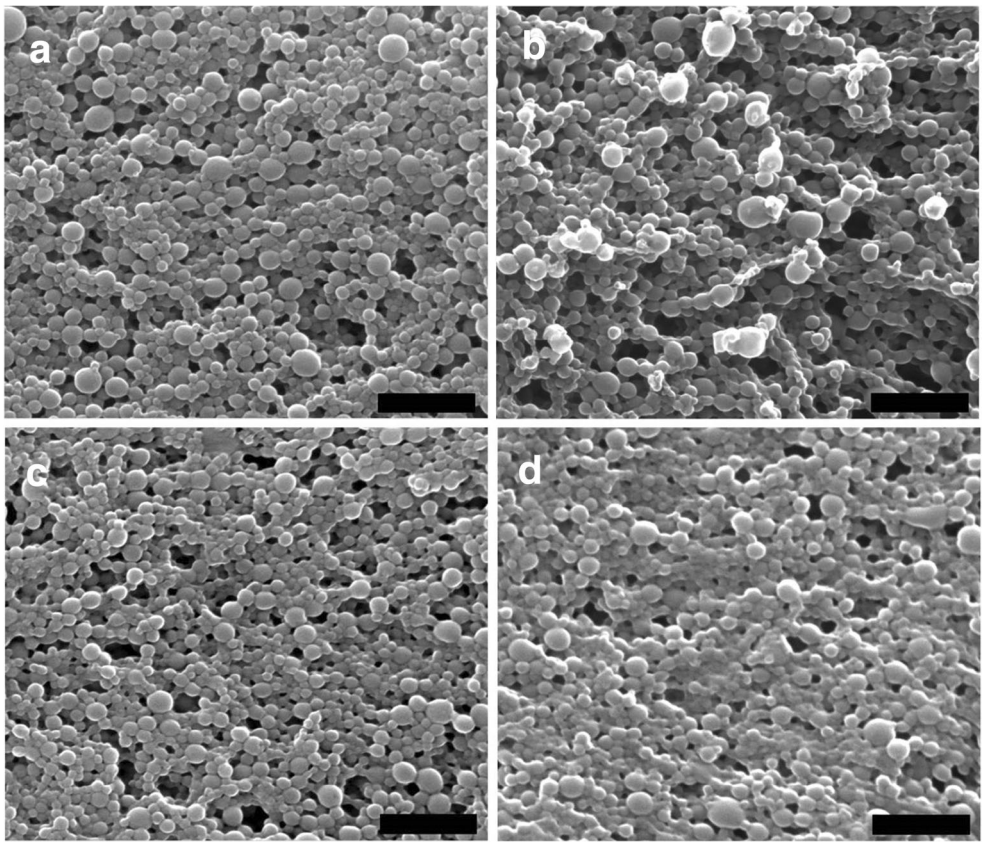

Fig. 1 Representative SEM images of empty (**a**) and RSV-loaded zein NPs with 5% (**b**), 10% (**c**), and 15% (**d**) theoretical DL. Scale bar = 500 nm

DL (Fig. 2a). The release of RSV from the polymer matrix may explain the decrease in NP size since this trend was not observed for unloaded NPs, discarding the possibility of NP degradation. However, the AE and DL did not confirm this explanation in full, since these values were only significantly affected in the case of 10% theoretical loading (Fig. 2d, c). The AE values in this last case decreased by around 6%. The ZP values did not significantly change in all types of NPs.

Zein NPs were freeze-dried and tested for their properties after re-dispersion in water. No cryoprotectants were used in

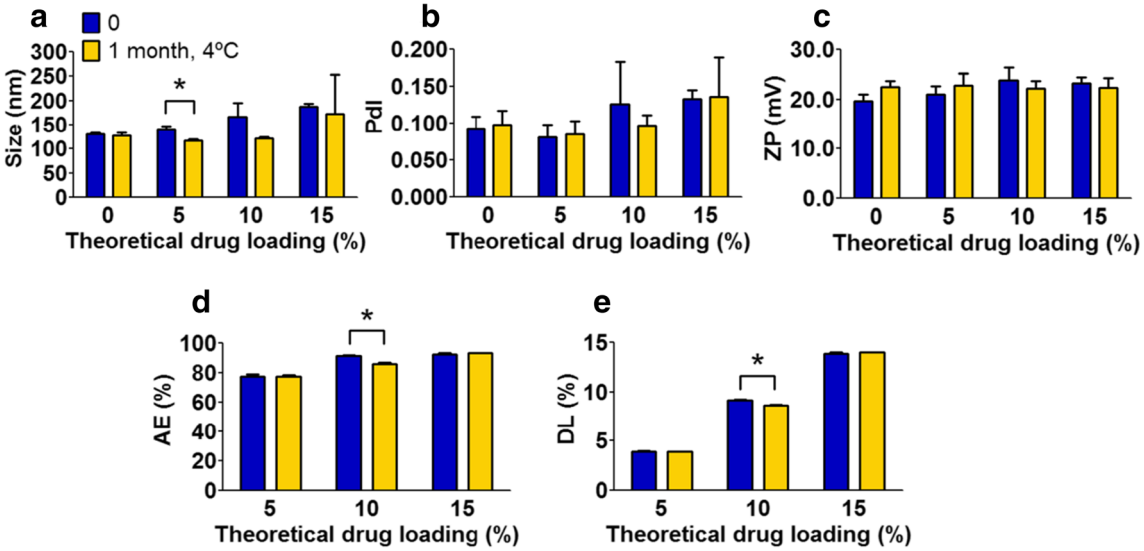

Fig. 2 Characteristics of resveratrol (RSV)-loaded zein nanoparticles (NPs) after production and after 30 days stored at 4 °C. Size expressed as hydrodynamic diameter (**a**), polydispersity index (PdI) (**b**), zeta potential (ZP) (**c**), association efficiency (AE) (**d**), and drug loading (DL) (**e**) of unloaded zein NPs (0% theoretical DL) and 5%, 10%, and 15% RSV-loaded zein nanoparticles. Bars present mean ± SD values ($n = 3$)

the first approach. After lyophilization, zein NPs were reconstituted in the initial volume of ultrapure water at a concentration of 1 mg mL^{-1}. The re-dispersion was difficult, resulting in the formation of visible aggregates that did not allow further DLS measurements. The aggregation of zein NPs during freeze-drying may be a consequence of increased hydrophobic interactions or physical entanglement of the protein [5]. The use of cryoprotectants may be an option to provide more stable formulations. Different sugars were tested in order to increase zein NP physical stability during the freeze-drying process, namely fructose, glucose, sucrose, and trehalose. The freeze-dried NPs obtained using the different cryoprotectants were visually inspected (Fig. 3). Glucose yielded a freeze-dried resembling a honeycomb-like structure (Fig. 3a) while the freeze-dried obtained using fructose matched a transparent resin (Fig. 3b). These features may be due to higher residual moisture content. Sucrose and trehalose freeze-dried NPs presented cotton candy–like texture, although more pronounced in the last case (Fig. 3c, d). Zein NPs were re-suspended in the same volume of water and characterized for their size and surface charge properties (Table 2). All cryoprotectants allowed complete re-suspension of zein NPs in water, contrasting with the case of zein NPs that were freeze-dried without cryoprotectants. However, none of the cryoprotectants was able to fully maintain the characteristics of the original dispersions of zein NPs. The mean diameter of zein NPs increased around 30 nm, 40 nm, 100 nm, and 150 nm when trehalose, sucrose, glucose, and fructose were used, respectively. PdI values were above 0.200 for all cryoprotectants, being the highest for fructose (PdI > 0.300). This suggests that mild aggregation occurred upon freeze-drying. The histogram relative to the intensity distribution of particle size clearly shows the presence of a second population of particles with a size above 4 μm (corresponding to approximately 3% of all NPs by intensity), indicating the presence of some aggregates in the samples (Figure S3, Supplementary information).

Overall, the best results were obtained when trehalose and sucrose were used as cryoprotectants for zein NPs, since the final size values remained closer to those initially determined. Taking into account these results, zein NPs containing different theoretical DL of RSV were lyophilized using sucrose as cryoprotectant. The size and surface charge properties of NPs after re-suspension in water are presented in Table 3.

Table 2 Hydrodynamic diameter (HD), polydispersity index (PdI) and zeta potential (ZP) values of RSV-loaded NPs after freeze-drying with no cryoprotectant or glucose, fructose, sucrose, or trehalose as cryoprotectants. Results are presented as mean ± SD ($n = 3$)

Freeze-drying	Cryoprotectant	HD (nm)	PdI	ZP (mV)
No	–	115 ± 1	0.153 ± 0.013	26.6 ± 1.9
Yes	None	ND	ND	ND
	Glucose	211 ± 10	0.283 ± 0.041	21.6 ± 1.2
	Fructose	269 ± 21	0.357 ± 0.044	20.0 ± 2.1
	Sucrose	155 ± 6	0.254 ± 0.031	19.0 ± 1.5
	Trehalose	147 ± 4	0.227 ± 0.027	18.8 ± 1.6

ND, not determined

Similar to what happened with unloaded NPs, mean hydrodynamic diameter values of the dispersions of NPs loaded with RSV experienced an increase of around 50 nm after freeze-drying with sucrose 10% (w/v) and re-suspension in water. The PdI values also were above 0.300, confirming the decrease in the size homogeneity of NP population. This suggests that mild aggregation occurred upon freeze-drying.

The in vitro drug release behavior of RSV-loaded zein NPs in PBS pH 6.8 was further performed. The cumulative amount of RSV (%) released over time using zein NPs immediately after production (liquid suspension), and lyophilized without cryoprotectant or with 10% (w/v) of sucrose is presented in Fig. 4. The release pattern of RSV from zein NPs was similar for all cases, showing a burst release in the first hour, followed by a plateau up to 24 h. However, the total amount of RSV released was different depending on the formulation used. In the case of fresh NPs, the amount of RSV released was around 20% of the initial amount, while this amount increased up to around 50–60%, for lyophilized NPs. These data suggest that lyophilization itself may increase the apparent permeability of RSV. One possible explanation for this phenomenon may be the increase in the porosity of the protein matrix after

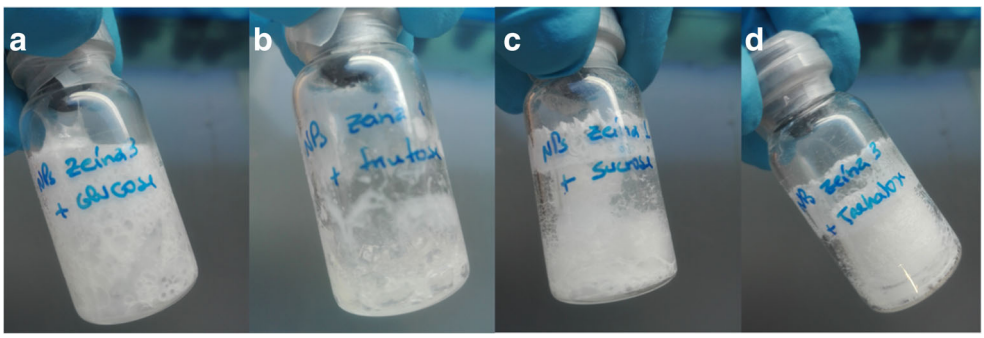

Fig. 3 Freeze-dried zein nanoparticles using different cryoprotectants (10% w/v). **a** Zein nanoparticles + glucose; **b** Zein nanoparticles + sucrose; **c** Zein nanoparticles + fructose; **d** Zein nanoparticles + trehalose

Table 3 Hydrodynamic diameter (HD), size distribution (PdI), and zeta potential of RSV-loaded zein NPs after freeze-drying with 10% (w/v) of sucrose and re-dispersion in water. Results are presented as mean ± SD ($n = 3$)

Theoretical drug loading (%)	HD (nm)	PdI	ZP (mV)
5	198 ± 11	0.309 ± 0.052	16.6 ± 6.6
10	215 ± 35	0.341 ± 0.073	22.2 ± 2.2
15	234 ± 45	0.303 ± 0.032	17.9 ± 2.2

lyophilization, as previously reported for polymers such as poly (lactic-*co*-glycolic acid) NPs [20], which could lead to increased exposure to the solute and enhance solubility. In the case of NPs lyophilized with sucrose, the increment of RSV released was even higher, around 40% regarding fresh NPs. The stabilization of NPs by sugar during freeze-drying processes is mainly achieved by the establishment of interactions between sugar molecules and the NPs, namely by hydrogen bonds. There are pieces of evidence that RSV binds spontaneously to proteins, not only by hydrophobic interactions but also by establishing hydrogen bonds [21, 22]. Inclusively, some studies suggest hydrogen bonds as the predominant interactions between zein and RSV rather than hydrophobic interactions [23]. So, one possible scenario may be the competition of sucrose and RSV for hydrogen bonds in the protein matrix, potentiating the release of RSV from the zein matrix. No differences were found in the release patterns of the NPs with different theoretical DL.

Cytotoxicity of RSV-loaded zein NPs

The ability of RSV-loaded zein NPs to affect the cell viability was assessed using two different models, namely the enterocyte-like Caco-2 cells and the mucin-producing HT29-MTX cells. Concentrations ranging from 0.1 to 1000 μM (expressed as the amount of drug) of free RSV and RSV-loaded zein NPs at different theoretical DL were incubated with the cells for 24 h. The results for cell viability are presented in Fig. 5. Zein NPs without RSV did not significantly affect the viability of both colorectal cell lines. In fact, viability values remained above the often considered lower viability threshold of 70% even for amounts higher than those used in experiments involving maximum concentrations of RSV (data not shown) [24]. The low cytotoxicity profile of zein is well described, thus making the case for its use as a safe matrix for drug delivery and tissue engineering purposes [25]. In fact, zein NPs were able to decrease the apparent toxicity of RSV, allowing an increase of the CC_{50} values of the drug from around 200 μM (173 μM for Caco-2 cells and 280 μM for HT29-MTX cells) to values higher than 1000 μM. The decrease in the viability of colorectal cell lines caused by free RSV seems to be in a dose-dependent manner, as previously reported [26]. The viability of both cell lines was close to 0 when concentrations of 1000 μm of free RSV were used. Overall, the use of RSV-loaded zein NPs appears to be at least as safe as the free drug.

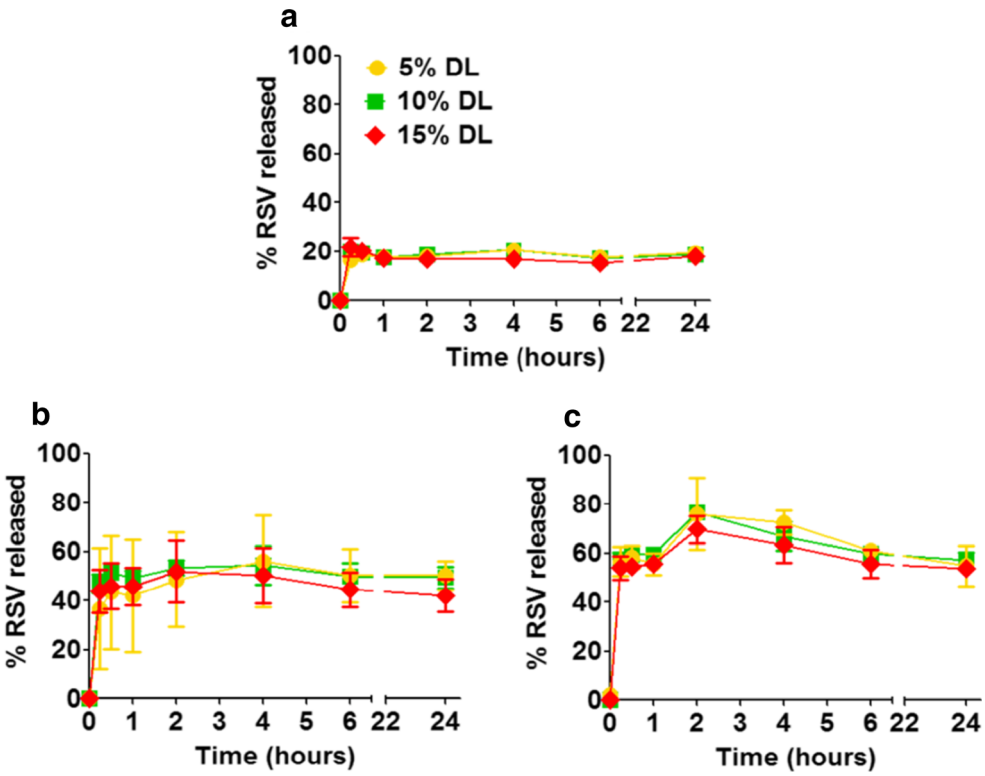

Fig. 4 In vitro release profile of RSV from zein NPs after production (**a**), freeze-drying without cryoprotectant (**b**), or using sucrose (10%, w/v) (**c**). Results are presented as mean ± SD ($n = 3$)

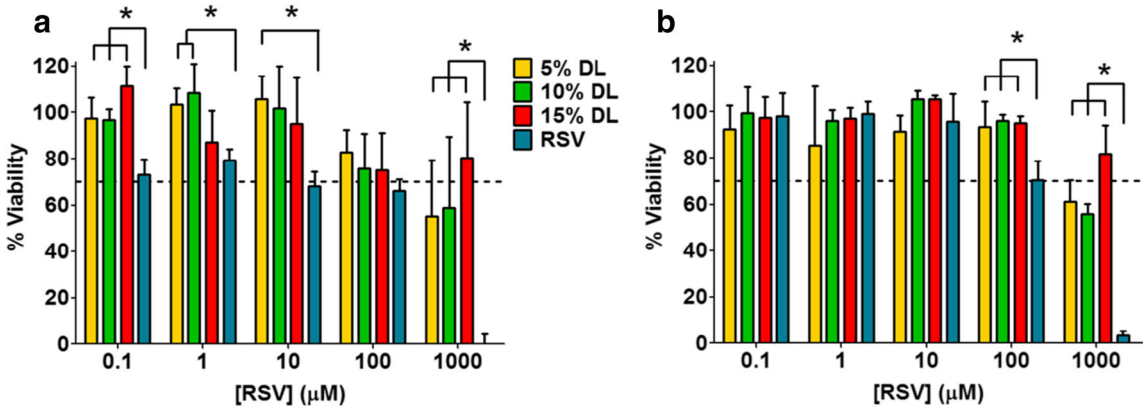

Fig. 5 Metabolic activity of Caco-2 cells (**a**) and HT29-MTX cells (**b**) after 24-h incubation with different concentrations of RSV-loaded zein NPs at different theoretical DL and free RSV, as assessed using the MTT metabolic activity assay. Results are presented as mean ± SD ($n = 3$). Asterisk denotes a significant difference ($p < 0.05$) when comparing equal concentrations of free RSV with RSV-loaded zein NPs at different theoretical DL

Permeability of RSV-loaded zein NPs across colorectal cell monolayers

The permeation of RSV-loaded zein NPs was conducted from apical to basolateral side in Caco-2 and Caco-2/HT29-MTX monolayers. NPs either in suspension or freeze-dried were tested and RSV permeability across Caco-2 and Caco-2/HT29-MTX cell monolayers monitored over 4 h. Figures 6 and 7 present the cumulative amount of RSV recovered from basolateral compartments when using fresh or freeze-dried zein NPs, respectively. The permeability of free RSV dispersed in HBSS with the aid of DMSO (final concentration of 0.1%, v/v) was tested for comparison purposes. The basolateral medium was added with the poloxamer 407 (0.2%, w/v) in order to assure sink conditions. The permeation profile of RSV across Caco-2 cell monolayers was very similar to that reported in the literature. RSV diffuses rapidly across Caco-2 cell monolayers, with reported P_{app} values between 10 and 20 × 10^{-6} cm s^{-1}, similar to those obtained in the present study (Tables 4 and 5) [27–29]. Regarding RSV-loaded zein NPs, different results were obtained depending on the state of the formulation used. In the case of NPs in suspension, used immediately after production, lower permeability of RSV was observed, which may reflect the limited RSV release from zein NPs, as previously shown in in vitro release studies (Fig. 4a). The difference between the permeability of RSV in solution and associated with zein NPs was around 40% in the Caco-2 cell monolayer model and 20% in the Caco-2/HT29-MTX cell monolayer model. Actually, P_{app} values for free RSV were reduced to half in the co-culture model compared with those obtained in Caco-2 cell monolayers, while in the case of NPs, the values were almost the same in the two models (Table 4). These findings may reflect the behavior of the free drug and zein NPs once in the presence of a mucus-like layer. Due to its hydrophobic character, RSV may be able to establish interactions with mucin produced in the co-culture cell monolayer model [30]. These interactions may partially impair the transport of the molecule

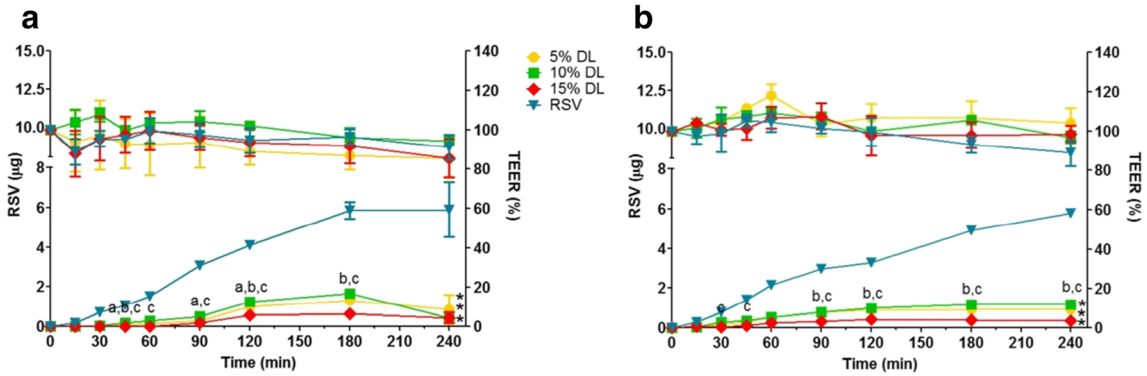

Fig. 6 In vitro cumulative permeability profile of RSV loaded in fresh zein NPs across Caco-2 (**a**) and Caco-2/HT29-MTX monolayers (**b**) and respective TEER (%) given as the percentage of the values prior to experiment (right *y*-axis). Results are presented as mean ± SD ($n = 3$). Asterisk denotes significant difference ($p < 0.05$) when compared with RSV in solution. Superscript letters a and b denote significant differences ($p < 0.05$) when 5% DL is compared with 10% DL or 15% DL, respectively, and superscript letter c when 10% DL is significantly different from 15% ($p < 0.05$)

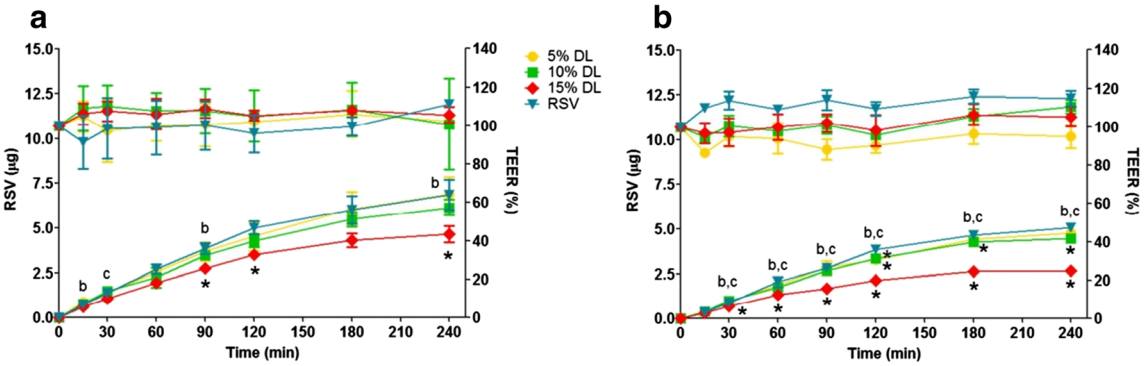

Fig. 7 In vitro cumulative permeability profile of RSV loaded in freeze-dried zein NPs across Caco-2 (**a**) and Caco-2/HT29-MTX monolayers (**b**) and respective TEER (%) given as the percentage of the values prior to experiment (right *y*-axis). Results are presented as mean ± SD ($n = 3$). Asterisk denotes significant difference ($p < 0.05$) when compared with RSV in solution. Superscript letters a and b denote significant differences ($p < 0.05$) when 5% DL is compared with 10% DL or 15% DL, respectively, and superscript letter c when 10% DL is significantly different from 15% ($p < 0.05$)

across the membrane and, consequently, reduce the likelihood to reach the basolateral compartment [31, 32]. Zein, despite being comprised mainly of hydrophobic amino acids, has also high glutamine content, conferring a certain hydrophilic surface to the particles [14, 33]. Furthermore, at the pH of the assay (7.4), zein NPs are negatively charged, which may allow certain repellence from negatively charged mucins [34–36]. In fact, previous multiple particle tracking studies (MPT) showed a better ability of plain zein NPs (although mucoadhesive) to diffuse in porcine intestinal mucus when compared with plain PLGA NPs [37]. The ability to better diffuse through the mucus may have dictated the lower difference between the permeability of free RSV and RSV-loaded zein NPs in the model containing mucus-producing cells. However, further investigation is needed.

The permeability profile of RSV from freeze-dried zein NPs was similar to the permeability of the free drug in both cell monolayers (Fig. 8). The more extensive release of the drug, as observed in in vitro studies (Fig. 5a-c) may explain these results. In this case, RSV levels increased faster in the basolateral compartment, possibly due to the higher amount of drug released from the NPs. This may also explain the attenuation of the differences in the permeability of free RSV and RSV from zein NPs in the co-culture model compared with Caco-2 cell monolayers. In all cases, the differences between the two cell monolayer models seem to highlight the importance of the interactions with mucin of both RSV and zein NPs in the overall permeability.

Overall and regardless of using fresh or freeze-dried NPs, the permeability profile of RSV was better when 5% or 10% DL NPs were used, with an advantage for 5% DL, as it can be confirmed by *P*app values (Tables 4 and 5). The increased amount of zein matrix for lower drug loadings may explain this finding since it is described that part of the N-terminal region of zein is able to interact with cell membranes, augmenting the likelihood of cell monolayer transposition [38]. An important aspect influencing the bioavailability of RSV is its poor stability, particularly due to enzymatic activity. Thus, we determine the total amount of drug recovered from the permeability system in order to estimate the possible degradation of the drug during experiments (Fig. 8). After 240 min, the total amount of RSV recovered from the apical and basolateral compartments, as well as from the cell monolayer, of the Caco-2 cell monolayer model was 100% for zein NPs

Table 4 Apparent permeability coefficient (P_{app}) values of RSV across Caco-2 and Caco/HT29-MTX cell monolayers for the free drug and fresh RSV-loaded NPs

	Caco-2 P_{app} (cm $s^{-1} \times 10^{-6}$)	Caco-2/HT29-MTX P_{app} (cm $s^{-1} \times 10^{-6}$)
5% DL	2.4 ± 2.1*	2.6 ± 0.2*[a,b]
10% DL	1.2 ± 0.1*	1.6 ± 0.2*[c]
15% DL	1.2 ± 0.7*	0.5 ± 0.0*
RSV	16.3 ± 3.8	8.0 ± 0.5

Results are presented as mean ± SD ($n = 3$). *Significant difference ($P < 0.05$) when compared with free RSV. [a],[b] Significant differences ($P < 0.05$) when 5% DL is compared with 10% DL or 15% DL, respectively. [c] When 10% DL is significantly different from 15% DL ($P < 0.05$)

Table 5 Apparent permeability coefficient (P_{app}) values of RSV across Caco-2 and Caco/HT29-MTX cell monolayers for the free drug and freeze-dried RSV-loaded NPs

	Caco-2 P_{app} (cm $s^{-1} \times 10^{-6}$)	Caco-2/HT29-MTX P_{app} (cm $s^{-1} \times 10^{-6}$)
5% DL	19.1 ± 2.6[b]	13.2 ± 2.6[b]
10% DL	17.1 ± 1.2	12.4 ± 1.8*[b]
15% DL	12.9 ± 1.3*	7.4 ± 0.1*
RSV	19.0 ± 2.3	13.7 ± 6.1

Results are presented as mean ± SD ($n = 3$). *Significant difference ($P < 0.05$) when compared with the free RSV. [a],[b] Significant differences ($P < 0.05$) when 5% DL is compared with 10% DL or 15% DL, respectively. [c] When 10% DL is significantly different from 15% ($P < 0.05$)

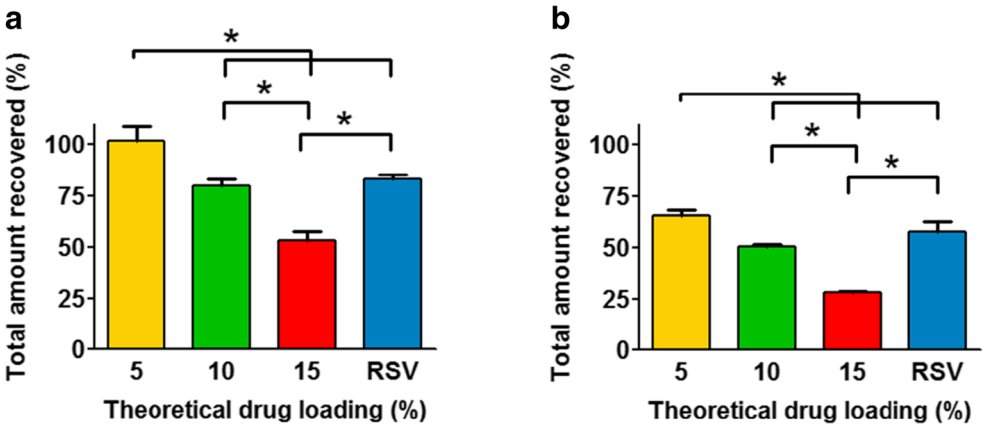

Fig. 8 Total amount of RSV (expressed as % of the initial amount added to the apical compartment) recovered from membranes, apical and basolateral compartments of Caco-2 (**a**) and Caco-2/HT29-MTX (**b**) models after permeability experiments. Results are presented as mean ± SD ($n = 3$). Asterisk denotes a significant difference ($p < 0.05$)

with 5% RSV DL (Fig. 8a), suggesting the ability of the NPs to protect RSV from intestinal cell-mediated metabolism. The recovery of RSV resulting from the permeability study of free RSV was less, around 80%, meaning that a considerable fraction was degraded. These values are consistent with those reported in the literature, namely the sulfation and, to a lesser extent, glucuronidation of around 13% of an initial concentration of RSV (50 μM) by Caco-2 cells after 4 h of incubation [26]. Curiously, zein NPs loaded with 10% and 15% presented only a recovery of around 75% and 50% of RSV. The explanation for these last values may be the presence of RSV adsorbed to the surface of NPs instead of being loaded within the protein matrix, thus exposing the drug prematurely. This is consistent with the usually reported loading capacity of less than 10% for zein NPs [39, 40]. Interestingly, the recovery values of RSV obtained for the Caco-2/HT29-MTX cell monolayer model were lower, resulting in around 70%, 60%, 50%, and 30% for 5% DL zein NPs, RSV in solution, 10% DL zein NPs, and 15% DL zein NPs, respectively (Fig. 8b). The lower recovery values of RSV obtained in this model may be due to the higher ability of the combination of Caco-2/HT29-MTX cells to metabolize the drug. In fact, the presence of HT29-MTX in the co-culture model was previously shown to modulate the metabolic activity of Caco-2 cells, namely by increased sulfation [41, 42].

Finally, the TEER values (Figs. 6 and 7, right *y*-axis) were maintained for all formulations, indicating that the integrity of cell monolayers throughout the experiments was not affected by free RSV and/or NPs [30]. This further reinforces the low cytotoxicity profile of zein NPs as shown in the MTT metabolic activity assay.

Conclusions

RSV-loaded zein NPs were successfully developed by using a simple nanoprecipitation technique. NPs presented suitable colloidal properties for oral drug delivery and high AE values and were stable over 1-month storage at 4 °C in aqueous suspension. The toxicity of RSV-loaded zein NPs to Caco-2 and HT29-MTX cells was shown to be low. Freeze-drying without the use of cryoprotectants caused considerable aggregation of zein NPs after re-suspension in water, while the use of 10% (w/v) sucrose seemed to reduce this effect. Freeze-drying of RSV-loaded zein NPs also resulted in more extensive drug release compared with fresh NPs. The permeability of RSV across Caco-2 and Caco-2/HT29-MTX cell monolayers seemed to be influenced by this effect. Fresh NPs led to reduced RSV transport across cell monolayers compared with the free drug, while freeze-dried counterparts showed similar permeability profiles to that of free RSV. Nevertheless, results from permeability studies suggest that zein NPs (particularly those with 5% theoretical DL) may have some impact on the metabolism of RSV by intestinal cells. The ability of zein NPs to protect RSV from enzymatic degradation processes may constitute an advantageous feature contributing to the oral bioavailability of RSV. Overall, the proposed RSV-loaded zein NPs present the potential to be used in the development of therapeutic or functional food products. Furthermore, the delayed release of the drug may also prolong the intestinal levels of RSV and contribute to more extensive absorption. Notwithstanding, freeze-drying processes need to be further investigated and optimized in order to allow more stable nanoformulations. Other issues, namely the interactions between zein and the intestinal mucus layer, deserve further investigation.

Funding information This work was financed by the project NORTE-01-0145-FEDER-000012 by Norte Portugal Regional Operational Programme (NORTE 2020) and COMPETE 2020 - Operacional Programme for Competitiveness and Internationalisation (POCI), under the PORTUGAL 2020 Partnership Agreement, through the FEDER - Fundo Europeu de Desenvolvimento Regional, and by Portuguese funds through FCT - Fundação para a Ciência e a Tecnologia/ Ministério da Ciência, Tecnologia e Ensino Superior in the framework of the project "Institute for Research and Innovation in Health Sciences" UID/BIM/04293/2019 and NETDIAMOND (POCI-01-0145-FEDER-016385). The authors acknowledge the support of the i3S Scientific Platforms Biointerfaces and Nanotechnology.

Compliance with ethical standards

Conflict of interest The authors declare that they have no conflict of interest.

References

1. Yu W, Fu YC, Wang W. Cellular and molecular effects of resveratrol in health and disease. J CellBiochem. 2012;113(3):752–9. https://doi.org/10.1002/jcb.23431.
2. Poulsen MM, Jørgensen JOL, Jessen N, Richelsen B, Pedersen SB. Resveratrol in metabolic health: an overview of the current evidence and perspectives. Ann N Y Acad Sci. 2013;1290(1):74–82. https://doi.org/10.1111/nyas.12141.
3. Neves AR, Lucio M, Lima JLC, Reis S. Resveratrol in medicinal chemistry: a critical review of its pharmacokinetics, drug-delivery, and membrane interactions. Curr Med Chem. 2012;19(11):1663–81. https://doi.org/10.2174/092986712799945085.
4. Amri A, Chaumeil JC, Sfar S, Charrueau C. Administration of resveratrol: what formulation solutions to bioavailability limitations? J Control Release. 2012;158(2):182–93. https://doi.org/10.1016/j.jconrel.2011.09.083.
5. Santos AC, Pereira I, Pereira-Silva M, Ferreira L, Caldas M, Collado-González M, et al. Nanotechnology-based formulations for resveratrol delivery: effects on resveratrol in vivo bioavailability and bioactivity. Colloids Surf B Biointerfaces. 2019;180:127–40. https://doi.org/10.1016/j.colsurfb.2019.04.030.
6. Fonte P, Araújo F, Silva C, Pereira C, Reis S, Santos HA, et al. Polymer-based nanoparticles for oral insulin delivery: revisited approaches. Biotechnol Adv. 2015;33(6, Part 3):1342–54. https://doi.org/10.1016/j.biotechadv.2015.02.010.
7. Majumder J, Taratula O, Minko T. Nanocarrier-based systems for targeted and site specific therapeutic delivery. Adv Drug Deliv Rev. 2019;144:57–77. https://doi.org/10.1016/j.addr.2019.07.010.
8. Soppimath KS, Aminabhavi TM, Kulkarni AR, Rudzinski WE. Biodegradable polymeric nanoparticles as drug delivery devices. J Control Release. 2001;70(1):1–20. https://doi.org/10.1016/S0168-3659(00)00339-4.
9. Almeida AJ, Souto E. Solid lipid nanoparticles as a drug delivery system for peptides and proteins. Adv Drug Deliv Rev. 2007;59(6):478–90. https://doi.org/10.1016/j.addr.2007.04.007.
10. Garícia-Fuentes M, Torres D, Alonso MJ. Design of lipid nanoparticles for the oral delivery of hydrophilic macromolecules. Colloids Surf B: Biointerfaces. 2003;27(2):159–68. https://doi.org/10.1016/S0927-7765(02)00053-X.
11. Elzoghby AO, Samy WM, Elgindy NA. Protein-based nanocarriers as promising drug and gene delivery systems. J Control Release. 2012;161(1):38–49. https://doi.org/10.1016/j.jconrel.2012.04.036.
12. Yin L, Yuvienco C, Montclare JK. Protein based therapeutic delivery agents: contemporary developments and challenges. Biomaterials. 2017;134:91–116. https://doi.org/10.1016/j.biomaterials.2017.04.036.
13. Rowe RC, Sheskey PP, Cook WG, Fenton ME. Handbook of pharmaceutical excipients, vol. 2. 7th ed. London: Pharmaceutical Press; 2013.
14. Paliwal R, Palakurthi S. Zein in controlled drug delivery and tissue engineering. J Control Release. 2014;189:108–22. https://doi.org/10.1016/j.jconrel.2014.06.036.
15. Anderson TJ, Lamsal BP. Zein extraction from corn, corn products, and coproducts and modifications for various applications: a review. Cereal Chem. 2011;88(2):159–73.
16. Vasconcelos T, Araújo F, Lopes C, Loureiro A, das Neves J. Marques S et al Multicomponent self nano emulsifying delivery systems of resveratrol with enhanced pharmacokinetics profile. Eur J Pharm Sci. 2019;137:105011. https://doi.org/10.1016/j.ejps.2019.105011.
17. Esen A. Separation of alcohol-soluble proteins (zeins) from maize into three fractions by differential solubility. Plant Physiol. 1986;80(3):623–7. https://doi.org/10.1104/pp.80.3.623.
18. Podaralla S, Perumal O. Influence of formulation factors on the preparation of zein nanoparticles. AAPS PharmSciTech. 2012;13(3):919–27. https://doi.org/10.1208/s12249-012-9816-1.
19. López-Nicolás JM, Garcia-Carmona F. Aggregation state and pKa values of (E)-resveratrol as determined by fluorescence spectroscopy and UV-visible absorption. J Agric Food Chem. 2008;56:7600–5.
20. Fonte P, Soares S, Costa A, Andrade JC, Seabra V, Reis S, et al. Effect of cryoprotectants on the porosity and stability of insulin-loaded PLGA nanoparticles after freeze-drying. Biomatter. 2012;2(4):329–39. https://doi.org/10.4161/biom.23246.
21. Acharya DP, Sanguansri L, Augustin MA. Binding of resveratrol with sodium caseinate in aqueous solutions. Food Chem. 2013;141(2):1050–4. https://doi.org/10.1016/j.foodchem.2013.03.037.
22. Hemar Y, Gerbeaud M, Oliver CM, Augustin MA. Investigation into the interaction between resveratrol and whey proteins using fluorescence spectroscopy. J Food Sci Technol. 2011;46(10):2137–44. https://doi.org/10.1111/j.1365-2621.2011.02728.x.
23. Joye IJ, Davidov-Pardo G, Ludescher RD, McClements DJ. Fluorescence quenching study of resveratrol binding to zein and gliadin: towards a more rational approach to resveratrol encapsulation using water-insoluble proteins. Food Chem. 2015;185:261–7. https://doi.org/10.1016/j.foodchem.2015.03.128.
24. ISO 10993-5:2009(2009) Biological evaluation of medical devices-part 5: tests for in vitro cytotoxicity.
25. Dong J, Sun Q, Wang J-Y. Basic study of corn protein, zein, as a biomaterial in tissue engineering, surface morphology and biocompatibility. Biomaterials. 2004;25(19):4691–7. https://doi.org/10.1016/j.biomaterials.2003.10.084.
26. Liu B, Zhou Z, Zhou W, Liu J, Zhang Q, Xia J, et al. Resveratrol inhibits proliferation in human colorectal carcinoma cells by inducing G1/Sphase cell cycle arrest and apoptosis through caspase/cyclinCDK pathways. Mol Med Rep. 2014;10(4):1697–702. https://doi.org/10.3892/mmr.2014.2406.
27. Yongmei L, Young Geun S, Chongwoo Y, Jerome WK, Wendy HH, John MP, et al. Increasing the throughput and productivity of Caco-2 cell permeability assays using liquid chromatography-mass spectrometry: application to resveratrol absorption and metabolism. Comb Chem High Throughput Screen. 2003;6(8):757–67. https://doi.org/10.2174/138620703771826865.
28. Kaldas MI, Walle UK, Walle T. Resveratrol transport and metabolism by human intestinal Caco-2 cells. J Pharm Pharmacol. 2003;55(3):307–12. https://doi.org/10.1211/002235702612.
29. Maier-Salamon A, Hagenauer B, Wirth M, Gabor F, Szekeres T, Jäger W. Increased transport of resveratrol across monolayers of the human intestinal Caco-2 cells is mediated by inhibition and saturation of metabolites. Pharm Res. 2006;23(9):2107–15. https://doi.org/10.1007/s11095-006-9060-z.
30. Araújo F, Sarmento B. Towards the characterization of an in vitro triple co-culture intestine cell model for permeability studies. Int J Pharm. 2013;458(1):128–34. https://doi.org/10.1016/j.ijpharm.2013.10.003.
31. Lechanteur A, das Neves J, Sarmento B. The role of mucus in cell-based models used to screen mucosal drug delivery. Adv Drug Deliv Rev. 2018;124:50–63. https://doi.org/10.1016/j.addr.2017.07.019.
32. Nunes R, Araújo F, Barreiros L, Bártolo I, Segundo MA, Taveira N, et al. Noncovalent PEG coating of nanoparticle drug carriers improves the local pharmacokinetics of rectal anti-HIV microbicides.

ACS Appl Mater Interfaces. 2018;10(41):34942–53. https://doi.org/10.1021/acsami.8b12214.
33. Dong F, Padua GW, Wang Y. Controlled formation of hydrophobic surfaces by self-assembly of an amphiphilic natural protein from aqueous solutions. Soft Matter. 2013;9(25):5933–41. https://doi.org/10.1039/C3SM50667C.
34. Gagliardi A, Paolino D, Iannone M, Palma E, Fresta M, Cosco D. Sodium deoxycholate-decorated zein nanoparticles for a stable colloidal drug delivery system. Int J Nanomedicine. 2018;13:601–14. https://doi.org/10.2147/ijn.s156930.
35. Lai S, Wang Y-Y, Hanes J. Mucus-penetrating nanoparticles for drug and gene delivery to mucosal tissues. Adv Drug Deliv Rev. 2009;61(2):158–71. https://doi.org/10.1016/j.addr.2008.11.002.
36. Macierzanka A, Rigby NM, Corfield AP, Wellner N, Böttger F, Mills ENC, et al. Adsorption of bile salts to particles allows penetration of intestinal mucus. Soft Matter. 2011;7(18):8077–84. https://doi.org/10.1039/C1SM05888F.
37. Inchaurraga L, Martínez-López AL, Abdulkarim M, Gumbleton M, Quincoces G, Peñuelas I, et al. Modulation of the fate of zein nanoparticles by their coating with a Gantrez® AN-thiamine polymer conjugate. Int J Pharm. 2019;1:100006. https://doi.org/10.1016/j.ijpx.2019.100006.
38. Fernández-Carneado J, Kogan MJ, Castel S, Giralt E. Potential peptide carriers: amphipathic proline-rich peptides derived from the N-terminal domain of γ-zein. Angew Chem Int Ed Engl. 2004;43(14):1811–4. https://doi.org/10.1002/anie.200352540.
39. Luo Y, Teng Z, Wang Q. Development of zein nanoparticles coated with carboxymethyl chitosan for encapsulation and controlled release of vitamin D3. J Agric Food Chem. 2012;60(3):836–43. https://doi.org/10.1021/jf204194z.
40. Lai LF, Guo HX. Preparation of new 5-fluorouracil-loaded zein nanoparticles for liver targeting. Int J Pharm. 2011;404(1):317–23. https://doi.org/10.1016/j.ijpharm.2010.11.025.
41. Poquet L, Clifford MN, Williamson G. Transport and metabolism of ferulic acid through the colonic epithelium. Drug Metab Dispos. 2008;36(1):190–7. https://doi.org/10.1124/dmd.107.017558.
42. Jailani F, Williamson G. Effect of edible oils on quercetin, kaempferol and galangin transport and conjugation in the intestinal Caco-2/HT29-MTX co-culture model. Food Funct. 2014;5(4):653–62. https://doi.org/10.1039/C3FO60691K.